EUROPEAN JOURNAL OF PURE AND APPLIED MATHEMATICS
2026, Vol. 19, Issue 1, Article Number 7243
ISSN 1307-5543 – ejpam.com
Published by New York Business Global

A Novel Study of Tumor-Immune-Microbiome with Cost Effective Analysis

Hanadi Alzubadi

Department of Mathematics, Umm Al-Qura University, Mecca 24382, Saudi Arabia

Abstract. The complex interplay among tumor cells, immune cells, and the microbiome has recently gained attention as a crucial determinant of cancer growth and treatment outcomes. In this work, a mathematical model has been developed and analysed to capture tumor-immune-microbiome interactions using a system of ordinary differential equations. It is explored how microbial species influence immune response and tumor growth dynamics. Applied analytical techniques reveal critical thresholds that govern tumor persistence. Moreover, an optimal control problem has been formulated, yielding effective therapeutic strategies that balance immune activation and microbiome modulation at the lowest treatment cost. The integrated approach provides novel insights into the mathematical foundation of the cancer-immune-microbiome system and explores sophisticated avenues for optimized cancer therapy.

2020 Mathematics Subject Classifications: 92D30, 34K13, 65L06

Key Words and Phrases: Mathematical model, Tumor-Immune interactions, Microbiome, Optimal Control, Cost-Effective Analysis.

1. Introduction

Cancer has become a severe worldwide epidemic and one of the top causes of death around the world. As it develops, cancer often gives rise to a mix of different tumor cells, making it harder to treat. This diversity is common in advanced stages of the disease [1]. Our understanding of how cancer cells grow, how to stop them, and how to destroy them is still very limited [2]. The body's immune system can recognize certain proteins on tumor cells and launch an attack, but it usually works best in the early stages– before medical treatment begins [3]. Even though new therapies are being developed, curing remains one of the toughest challenges in modern medicine [4]. Protecting healthy cells while fighting cancer throughout the body is also important. Traditional methods like surgery, chemotherapy, and radiotherapy often fall short because treatment plans aren't always well-targeted [5]. That's why there is a strong need for new and smarter treatment strategies to improve long-term results.

DOI: https://doi.org/10.29020/nybg.ejpam.v19i1.7243

Email address: hhzubadi@uqu.edu.sa (H. Alzubadi)

Biomedical research is increasingly focusing on the intestinal microbiome, which has a profound impact on both health and disease. Alterations in the composition and metabolic functionality of intestinal microbiota have been consistently associated with heightened susceptibility to immune-related disorders, including inflammatory bowel disease, autoimmune conditions, chronic inflammation, and various cancers [6]. Recent investigations have explored the potential link between gut microbial communities and the therapeutic outcomes and toxicities associated with immune checkpoint inhibitor(ICI) immunotherapy. Foundational evidence was provided by a seminal pre-clinical study by Sivan et al., which demonstrated that enrichment of Bifidobacterium species in the gut microbiota correlated with delayed tumor progression, increased T-cell infiltration into tumors, and enhanced anti-tumor immune responses, thereby improving the efficiency of PD-L1 blockade [7]. Since then, numerous pre-clinical and clinical studies have aimed to elucidate the causal relationships between distinct microbial signatures and patient responsiveness to ICI treatments [8].

Microbial species can be integrated into cancer treatment through innovative strategies that enhance immune responses and improve therapeutic outcomes. One common method is probiotics, where beneficial bacteria such as Bifidobacterium or Lactobacillus are administered orally to support gut health and boost the immune system, thereby enhancing the effectiveness of treatments like immune checkpoint inhibitors (ICIs). Fecal microbial transplant **(FMT)** involves transplanting stools from a healthy donor into a patient's bowel to change their microbiome and enhance cancer treatment response. Genetically engineered bacteria are also being developed to deliver therapeutic agents directly to tumors, stimulating targeted immune activity. Additionally, dietary interventions rich in fiber and prebiotics can naturally promote beneficial microbial growth. Finally, researchers are investigating how microbiome-derived compounds like fatty acids with short chains can alter the immune pathway and improve cancer treatment [9].

Mathematical modeling is the process of creating and evaluating mathematical representations of real-world phenomena [10, 11]. The conceptual model figures out the important variables, parameters, and principles that describe how they relate to one another [12, 13]. It is an essential tool in many scientific and engineering fields. It also plays an important role in epidemiology [14, 15]. A mathematical model uncovers basic dynamical principles that are difficult to analyze through simple observations. Many researchers have used mathematical modeling to examine various diseases and social behaviors. Awan *et al.* analyzed pine wilt disease in pine trees through a deterministic mathematical model [16]. Ozair *et al.* also analyzed this disease through the assumption of an asymptomatic carrier in pine trees [17]. The menace of smoking has been explored through a mathematical model by Hussain *et al.* [18]. Many authors have employed classical tumor-growth models to describe tumor dynamics. Szabo and Merks observed tumor growth, invasion, and progression using a cellular Potts Model [19]. Tumor growth has been studied by Zuppone *et al.* in Mouse models of bladder cancer [20]. To estimate the minimum radiation dose for tumor control, *Kutuva et al.* developed and analyzed a mathematical model.

Recently, many researchers have developed mathematical models to study interactions between tumor cells and the immune system, thereby enabling the design of effective therapeutic strategies. Kim *et al.* studied tumor-immune interactions using a mathematical model that considers the role of a PD-L1 inhibitor [21]. To provide deep insight into tumor growth analysis, Unni and Seshaiyer developed a compartmental model that assumes drug delivery to natural killer cells, dendritic cells, and cytotoxic cells [22]. In the study of tumor-immune dynamics, Song *et al.* focused on the natural killer cells and cytotoxic lymphocytes in immune surveillance [23]. Das *et al.* formulated an optimal control problem with treatments as control measures. The authors explained the circumstances through which cancerous cells can be destroyed [24]. Dhar *et al.* developed a tumor-immune model and analyzed the dosage effect of targeted chemotherapeutic drugs on the abnormal size of beginning tumors [25].

The impact of impulsive therapy was studied by Sardar *et al.* through a mathematical model in tumor-immune interactions [26]. The application of radio-chemotherapy was carried out by Kumar *et al.* through a mathematical model [27]. The interactions among tumor-immune-healthy cells and stored fat in the body were examined by Qin *et al.* [28]. It has been demonstrated that fractionally ordered models offer an effective means of simulating intricate disease processes. In fact, a fractional tumor–immune–vitamins model was put forth in [29], in which it was found that fractional controllers and vitamin interventions have a major impact on cancer suppression. In [30], an analogous model for fraction HBV was provided utilising the Caputo using Atangana-Baleanu derivatives, highlighting the function of calculus of fractions and numerical methods in epidemiology. The aforementioned research has inspired us to examine tumor-autoimmune interactions in more detail within the structure of mathematical modelling. The importance of irregular and fractionally ordered frameworks in comprehending complicated biological systems is shown by the latest advancements in illness modelling. In addition to fractional virus infection models that include immune system responses as well as cure processes [31], vaccine-based COVID-19 simulations were previously examined employing a bifurcation evaluation method [32]. Recently, partial-order cholera frameworks have been discussed in terms of dynamical behaviour and computational simulations [33]. These publications inspire the current work and demonstrate the effectiveness of contemporary mathematical techniques in disease modelling.

To the best of my knowledge, the analytical and numerical impact of different therapies on microbes, however, has not been well studied. Thus, I present a mathematical model to investigate tumor responses to concurrent therapies involving microbiota.

2. Mathematical Model

The mathematical model outlined here consists of three populations: tumor, immune, and microbiome, as well as the levels of drugs throughout the human body. The system

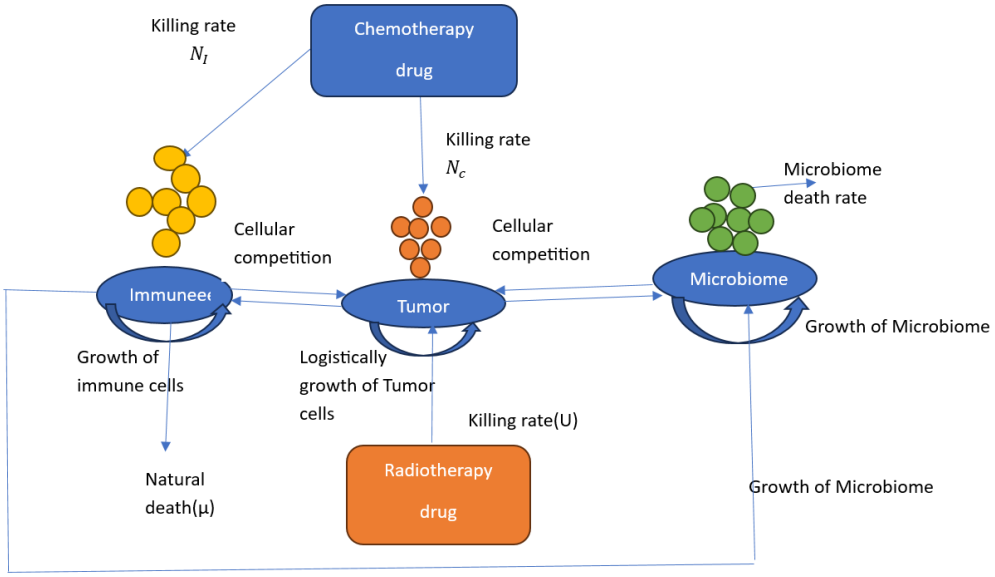

Figure 1: Flow Chart

of ordinary differential equations representing cancer disease is as follows:

$$\begin{aligned}
\frac{dT}{dt} &= rT\left(1-\frac{T}{K_T}\right)-\beta TI-N_T\left(1-e^{-P}\right)T-\gamma TM-UT,\\
\frac{dI}{dt} &= \frac{\alpha IT}{T+K_I}-\phi IT-\mu I-N_I\left(1-e^{-P}\right)I,\\
\frac{dM}{dt} &= \delta-\eta M+\theta I,\\
\frac{dU}{dt} &= -\chi U+\zeta,\\
\frac{dP}{dt} &= -\sigma P+q,
\end{aligned} \tag{1}$$

where $T(0)\geq 0, I(0)\geq 0, M(0)\geq 0, U(0)\geq 0,$ and $P(0)\geq 0$. The flow Diagram of the model is shown in Figure 1. In the model (1), $T(t)$ denotes as the quantity of tumor cell, $I(t)$ refers to the quantity of immune cell within the single compartment, $M(t)$ is microbiome, $U(t)$ is the amount of radiotherapy and $P(t)$ is the amount of chemotherapy. The first equation of the mathematical model (1) provides a rate of change for the tumor cell community over the period t. This equation's initial term, independent of other population variables, describes the logistic growth of cancerous cells, with a development rate r and a maximal carrying capacity K_T. The symbol β denotes the rate at which immune system cells $I(t)$ eliminate tumor cells. The drug is thought to destroy every kind of cell. Medication, including doxorubicin, cisplatin, and others, is being used to target the kidneys, lungs, and breast cancer. The simulation includes a variable that accounts for radio- and chemotherapy-induced cell death in every single cell community equation. Certain chemotherapy drugs, such as doxorubicin, act only at specific phases of the cell cycle,

while pharmacokinetics suggests chemo's effectiveness is limited. Consequently, fractional cells are killed by chemotherapeutic means with a saturating period of $(1 - e^{-p})$.

At relatively low dosages of drugs, the death rate is nearly linear, and at increasing drug concentrations, it plateaus. I believe that although the medication kills all cell types, the rate of death differs depending on the groups. An exponential response curve is used to stimulate it. For a given quantity of medication, q, let $F(u)$ represent the proportion of cells destroyed at the tumor site. The provided dosage q and the medication's overall mortality rate σ affect $P(t)$. Pillis et al. [34], using the equation $F(N_\omega, P) = (1 - e^{-p})N_\omega$to eliminate cells in a specific location in the tumor by a specific medication dosage. During this initial inquiry, they put $k = 1$ in this exploratory study. The mathematical formula used here is consistent with the dosage response curve reported in previous research [35].

The reaction equation $F(N_\omega, P) = (1-e^{-p})N_\omega$ at $\omega = T, I$ are so expressed. N_T along with N_I are two reaction coefficients that area being introduced. The conflict between cancerous cell $T(t)$ and microbiome $M(t)$ results in a reduction of tumor cell populations, which is referred to as γ. The evaluation of the immune system cell populations over a period t is depicted by the second equation of system (1). The mechanism is simulated by the tumor-specific antigens produced by the cancerous cells, as indicated by the first component of that equation. Their antigenicity determines the speed of immune recognition of tumor cells. The regional growth rate, plus the influx to killing cells, is shown by the term $\frac{\alpha IT}{T+K_I}$. The community antigenicity of cancerous cells, K_I, induces cytokines that respond to cytokine vaccination signals. I hypothesize that the number of tumor cells with positive values of K_I and α influences the induction of the body's immune system, given the complexity of the detection procedure. Immune system cells died naturally at a rate of μ, while tumor cells inactivate antibodies at a speed of ϕ. I consider η to be the body's death ratio and δ to be the microbe's growth rate. The effect of antibodies on the structure of the microbiota is reflected by the θ. I assumed the situation in which the presence of immune cells correlates with microbiome. Immune cells reduce the tumor burden and the smaller size tumor may no longer supress the microbiota. Thus the net effect of increasing the immune cells is positive for the microbiome. The rate of shift in radioactive medications is depicted in the 4^{th} equation in system (1). In this case, χ stands for the drug's decay rate and α for the dosage of radiation medication.

3. Positivity and Boundedness

Theorem 1. *In the region* $R_+^5 = \{(T, I, M, U, P) : T, I, M, U, P \in R_+\}$ *for every time* $t \geq 0$*, all the solutions of model (1) stay positive, and all its initial conditions are also positive.*

Proof: As the simulation system (1)'s rightmost side is continuous, it satisfies the regional Lipschitz condition. The solution (T, I, M, U, P) of model (1) exists for the given initial conditions. The first two equations of model (1) can be written as follows:

$\frac{dT}{dt} = T\phi_1(T,I,M,U,P)$, $\frac{dI}{dt} = I\phi_2(T,I,M,U,P)$,
where
$\phi_1 = r\left(1-\frac{T}{K}\right) - N_T\left(1-e^{-P}\right) - \beta I - \gamma M - U, \quad \phi_2 = \frac{\alpha T}{T+K_I} - \mu - N_I\left(1-e^{-P}\right)$.
It follows that
$T(t) = T(0)e^{\int_0^t \phi_1(T(\theta),I(\theta),M(\theta),U(\theta),P(\theta))d\theta} \geq 0, \quad I(t) = I(0)e^{\int_0^t \phi_2(T(\theta),I(\theta),M(\theta),U(\theta),P(\theta))d\theta} \geq 0$.
The third equation of model (1) gives us
$M = \frac{\delta}{\eta}\left(M(0) - \frac{\delta}{\eta}\right)e^{-\eta t} + \theta I(0)e^{\int_0^t \phi_2(T(\theta),I(\theta),M(\theta),U(\theta),P(\theta))d\theta \geq 0}$.
To the $4th$ equation of system (1), I obtain
$U = \frac{\zeta}{\beta} + (U(0) - \frac{\zeta}{\beta})e^{-\beta t} \geq 0$.
Using last equation of cancerous model (1), then
$P = \frac{q}{\sigma} + (P(0) - \frac{q}{\sigma})e^{-\sigma t} \geq 0$.
Therefore, all the solutions of $I(t), I(t), M(t), U(t)$,and $P(t)$ are positive $\forall t \geq 0$, then $T(0) \geq 0, I(0) \geq 0, M(0) \geq 0, U(0) \geq 0, P(0) \geq 0$.

Theorem 2. *Every solution of the model (1) that starts in R_+^5 and will stay contained in its attractive zone*
$\Omega = \{(T,I,M,U,P) \in R_+^5 : 0 \leq T \leq K_T, 0 \leq I \leq K_T, M(t) \leq \max\left(M(0), \frac{(\delta+\theta K_T)}{\eta}\right),$
$U \leq \max\left(U(0), \frac{\alpha}{\gamma}\right), P \leq \max\left(P(0), \frac{q}{\sigma}\right)\}$.

Proof: It may easily deduce to the first expression of the system (1) that $\frac{dT}{dt} \leq rT\left(1-\frac{T}{K_T}\right)$, implying as $lim_{t\to\infty} \sup T(t) \leq K_T$
Now suppose $L = T + I$, then it becomes
$\frac{dL}{dt} = \frac{dT}{dt} + \frac{dI}{dt} \leq rT - \frac{rT^2}{K_T} + I\left(\frac{\alpha T}{T+K_I} - \phi T\right) - \mu I$.

Let $g(T) = \frac{\alpha T}{T+K_I} - \phi T$, then g has maximum value g_{max} at $T = \sqrt{\frac{\alpha K_I}{\phi}} - K_I$. Here $T > 0$ if $\frac{\alpha}{\phi} > K_I$. Hence, it follows

$\frac{dL}{dt} \leq rT - \frac{rT^2}{K_T} - (\mu - g_{max})I$,where $\mu > g_{max}$ and $\mu - g_{max} = \mu^*$,
$\leq rT - \frac{rT^2}{K_T} - \mu^* I$,
$\leq 2rT - \delta^* L - \frac{rT^2}{K_T}$,
where $\delta^* = min\{r, \mu^*\}$, which implies
$\frac{dL}{dt} + \delta^* L \leq 2rT - \frac{rT^2}{K_T}$.
Let $f(T) = 2rT - \frac{rT^2}{K_T}$, then f has maximum value $f_{max} = rK_T$ at $T = K_T$.
$limsup_{t\to\infty} L(t) \leq \frac{rK_T}{\delta^*}$.

However, it can be inferred from the remaining equations of model (1) as
$M(t) \leq \max\left(M(0), \frac{rK_T}{\delta^*}\right), U(t) \leq \max\left(\frac{\alpha}{\gamma}, U(0)\right)$ and $P(t) \leq \max\left(\frac{q}{\sigma}, P(0)\right)$.

As a result, I can infer that all of the system solutions of system (1) that starts inside R_+^5 are confined to the region Ω.

4. Equilibrium Points of the Model:

Fixed points of the model (1) can be acquired by placing

$$\frac{dT}{dt} = 0 \Longrightarrow \left\{T = 0 \quad T = \frac{K_T\left(r-\beta I-N_T\left(1-e^{-P}\right)-\gamma M-U\right)}{r}. \right. \tag{2}$$

$$\frac{dI}{dt} = 0 \Longrightarrow \left\{I = 0 \quad \frac{\alpha T}{T+K_I} - \phi T - \mu - N_I\left(1-e^{-P}\right) = 0. \right. \tag{3}$$

$$\frac{dM}{dt} = 0 \Longrightarrow M = \frac{\delta + \theta I}{\eta}. \tag{4}$$

Here, on simplification, I get

$$T^2 + \left(K_I + \frac{\mu + N_I\left(1-e^{-P}\right) - \alpha}{\phi}\right)T + \mu K_I + KN_I\left(1-e^{-P}\right) = 0. \tag{5}$$

Further

$$\frac{dU}{dt} = 0 \Longrightarrow U = \frac{\zeta}{\beta}, \tag{6}$$

$$\frac{dP}{dt} = 0 \Longrightarrow P = \frac{q}{\sigma}. \tag{7}$$

The following three physiologically relevant equilibrium points can be determined by solving the equation:

1. The initial point that results from the extensive application of therapy if no one of the cells are affected the population, $E_1 = \left(0, 0, \frac{\delta}{\eta}, \frac{\zeta}{\beta}, \frac{q}{\sigma}\right)$.

2. The second equilibrium point is obtained as $E_2 = \left(\bar{T}, 0, \frac{\delta}{\eta}, \frac{\zeta}{\beta}, \frac{q}{\sigma}\right)$, that is $\bar{T} = \frac{\left(r-N_T\left(1-e^{-P}\right)-\frac{\gamma\delta}{\eta}-\frac{\zeta}{\beta}\right)K_T}{r}$, $r \geq N_T\left(1-e^{-P}\right) + \frac{\gamma\delta}{\eta} + \frac{\zeta}{\beta}$. It indicates that the tumor cells have been detected at an optimal level.

3. The presence of malignant cells in the model causes immune cell types to remain due to their antigenicity, meaning both of them exist jointly, as indicated by this third equilibrium level $E_3 = \left(\hat{T}, \hat{I}, \hat{M}, \frac{\zeta}{\beta}, \frac{q}{\sigma}\right)$. Here

$r\hat{T}\left(1-\frac{\hat{T}}{K_T}\right) - \beta\hat{T}\hat{I} - N_T\left(1-e^{-P}\right)\hat{T} - \gamma\hat{T}\hat{M} - \hat{U}\hat{T} = 0,$

$\hat{I} = \frac{1}{\beta}\left(r - \frac{r\hat{T}}{K_T} - N_T\left(1-e^{-\frac{q}{\sigma}}\right) - \gamma\frac{\delta}{\eta} - \frac{\zeta}{\beta}\right),$

$\hat{M} = \frac{\delta}{\eta} + \frac{\theta}{\eta\beta}\left(r - \frac{r\hat{T}}{K_T} - N_T\left(1-e^{-\frac{q}{\sigma}}\right) - \gamma\frac{\delta}{\eta} - \frac{\zeta}{\beta}\right),$

and $\hat{T}$ is the solution of the equation given below:

$A_1\hat{T}^2 + A_2\hat{T} + A_3 = 0,$

where

$A_1 = 1, A_2 = \left(K_I + \frac{\mu+N_I\left(1-e^{-\frac{q}{\sigma}}\right)-\alpha}{\phi}\right),$ and $A_3 = \mu K_I + KN_I\left(1-e^{-\frac{q}{\sigma}}\right).$

Further the roots $\hat{T}$ can be written as
$\hat{T} = \frac{-A_2 \pm \sqrt{A_2^2 - 4A_3}}{2}$.
The Equilibrium point E_3 possible if
$A_2 < 0 \implies \alpha > \phi K_I + \mu + N_I \left(1 - e^{-\frac{q}{\sigma}}\right) = \alpha^{thresh}$,
$\hat{T} < \frac{K_T\left(r - N_T\left(1 - e^{-\frac{q}{\sigma}}\right) - \gamma\frac{\delta}{\eta} - \frac{\zeta}{\beta}\right)}{r} = T_T$,
$A_2^2 - 4A_3 > 0 \Longrightarrow \left(K_I + \frac{\mu + N_I\left(1 - e^{-\frac{q}{\sigma}}\right) - \alpha}{\phi}\right)^2 > 4\mu K_I + KN_I\left(1 - e^{-\frac{q}{\sigma}}\right)$.

To fend off a tumor attack, the development rate of tumor cells must be above α^{thresh}, and the tumor cells should be under a particular threshold level, T_T.

When E_3 is reduced to E_2 at $\hat{T} = \frac{K_T\left(r - N_T\left(1 - e^{-\frac{q}{\sigma}}\right) - \gamma\frac{\delta}{\eta} - \frac{\zeta}{\beta}\right)}{r}$, an equilibrium indicate that cancerous cells are always present in a infected person's bloodstream.

5. Stability of Equilibria

To obtain the local stability of equilibria, I calculate the Jacobian matrix as follows:

$$\begin{bmatrix} j_{11} & -T\beta & -T\gamma & -T & -TN_T e^{-P} \\ j_{21} & j_{22} & 0 & 0 & -IN_I e^{-P} \\ 0 & \theta & -\eta & 0 & 0 \\ 0 & 0 & 0 & -\chi & 0 \\ 0 & 0 & 0 & 0 & -\sigma \end{bmatrix}, \tag{8}$$

where

$$\begin{aligned} j_{11} &= -\frac{1}{K_T}\left(UK_T - rK_T + K_T N_T + 2rT + I\beta K_T + M\gamma K_T - K_T N_T e^{-P}\right), \\ j_{21} &= \frac{I}{(T + K_I)^2}\left(\phi T^2 + 2\phi T K_I + \phi K_I^2 - \alpha K_I\right), \\ j_{22} &= -\frac{1}{T + K_I}\left(T\mu - T\alpha + TN_I + \mu K_I + K_I N_I + T^2\phi + T\phi K_I - TN_I e^{-P} - K_I N_I e^{-P}\right). \end{aligned}$$

At the equilibrium point, $E_1\left(0, 0, \frac{\delta}{\eta}, \frac{\zeta}{\beta}, \frac{q}{\sigma}\right)$, the eigenvalues are $-\sigma, -\chi, -\eta$, $-\frac{1}{K_T}\left(\frac{\zeta}{\beta}K_T - rK_T + K_T N_T + \frac{\delta}{\eta}\gamma K_T - K_T N_T e^{-\frac{q}{\sigma}}\right), -\frac{1}{K_I}\left(\mu K_I + K_I N_I - K_I N_I e^{-\frac{q}{\sigma}}\right)$. Thus E_1 is asymptotically stable if $\frac{\zeta}{\beta} + \frac{\delta}{\eta}\gamma + N_T\left(1 - e^{-\frac{q}{\sigma}}\right) > r$ and $\sigma \ln\left(\frac{N_I}{\mu + N_I}\right) > q$, otherwise it is unstable. For the equilibrium point $E_2\left(\bar{T}, 0, \frac{\delta}{\eta}, \frac{\zeta}{\beta}, \frac{q}{\sigma}\right)$, the eigenvalues are $-\sigma, -\chi, -\eta$, $-\frac{1}{K_T}\left(\frac{\zeta}{\beta}K_T - rK_T + K_T N_T + 2r\bar{T} + \frac{\delta}{\eta}\gamma K_T - K_T N_T e^{-\frac{q}{\sigma}}\right)$, $-\frac{1}{T + K_I}\left(\bar{T}\mu - \bar{T}\alpha + \bar{T}N_I + \mu K_I + K_I N_I + \bar{T}^2\phi + \bar{T}\phi K_I - \bar{T}N_I e^{-\frac{q}{\sigma}} - K_I N_I e^{-\frac{q}{\sigma}}\right)$. This equilibrium point is asymptotically stable under the condition $r < 2\left(N_T\left(1 - e^{-\frac{q}{\sigma}}\right) + \frac{\gamma\delta}{\eta} + \frac{\zeta}{\beta}\right)$

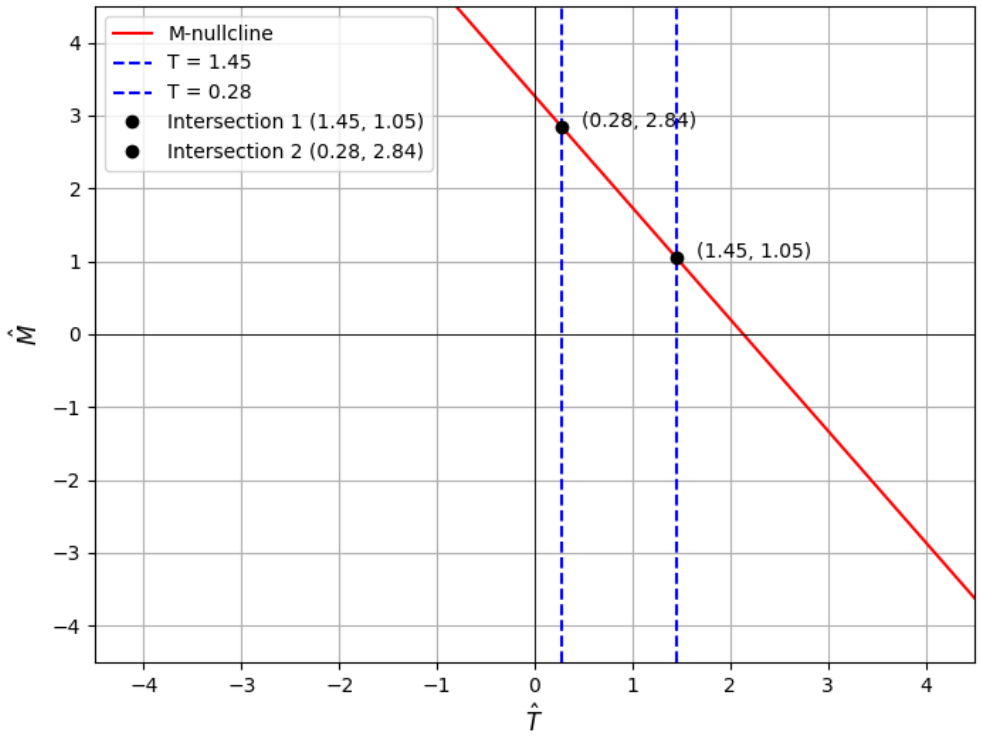

Figure 2: Plot for interior equilibria

and $\alpha < \mu + \bar{T}\phi + \phi K_I + \frac{K_I}{\bar{T}}\left(\mu + \left(\bar{T} + K_I\right)\left(1 - e^{-\frac{q}{\sigma}}\right)\right)$.

Example: To obtain positive equilibria, I numerically solve the equations (2)-(7) in terms of $\hat{T}$ and $\hat{M}$. Using $r = 1, K_T = 1, N_T = 0.9, \zeta = 0.0001, \beta = 0.8, \gamma = 0.082, q = 0.0064, \sigma = 0.9, \delta = 1.0, \theta = 0.7, \eta = 0.5, K_I = 1, \mu = 0.4, N_I = 0.9, \alpha = 4.5, \phi = 1.5$, I get two equilibria as shown in Figure 2. Given these values for parameter, the condition $r = 1 \geq N_T\left(1 - e^{-P}\right) + \frac{\gamma\delta}{\eta} + \frac{\zeta}{\beta} = 0.329$ is satisfied. Figure 3 represents the surface map for this set of parameter values.

6. Optimal Control

By defining the optimum control dilemma, the main objective is to reduce the size of the tumor with the minimum cost of application of radiotherapy and chemotherapy. The other purpose is to minimize the negative impact of these therapies on the microbial population. Furthermore, our goal is to apply optimal control theory to develop an effective treatment strategy. It is an example of a situation in which both radiation and chemotherapy, along with strategies to kill bacteria, can be used in tandem to provide a more effective treatment

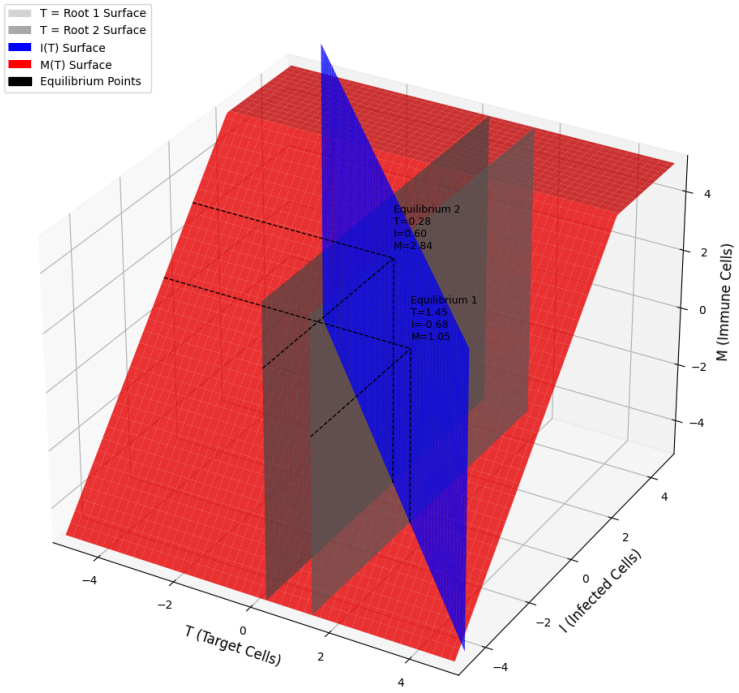

Figure 3: Surface plot of model (1)

plan that prevents infection and cancer. Examine the mathematical model (1) which has $\zeta = u_2,\ q = u_3$ also by adding u_1 as stated:

$$\begin{aligned}
\frac{dT}{dt} &= rT\left(1 - \frac{T}{K_T}\right) - \beta TI - N_T(1 - e^{-P})T - \gamma TM - UT,\\
\frac{dI}{dt} &= \frac{\alpha IT}{T + K_I} - \phi IT - \mu I - N_I(1 - e^{-P})I,\\
\frac{dM}{dt} &= \delta - \eta M + \theta I - u_1(t)M,\\
\frac{dU}{dt} &= -\chi U + u_2(t),\\
\frac{dP}{dt} &= -\sigma P + u_3(t).
\end{aligned} \tag{9}$$

Mathematical model (1) initial conditions apply to the system (9) conditions. Our goals are to protect the patients throughout treatment, optimize the formation of immune effector cells, reduce the spread of cancerous cells, while controlling any negative pharmaceutical

adverse effects and medication expenses. I establish a cost function that must be decreased to do this.

$$J(u_1(t),\ u_2(t),\ u_3(t)) = \int_0^T \left[T - M + \frac{1}{2}\left(w_1 u_1^2 + w_2 u_2^2 + w_3 u_3^2\right)\right] dt. \tag{10}$$

The weighted variables $w_1,\ w_2,$ and w_3 indicates the significance of therapy control, taking into consideration the amount of medication toxicities in the human body, as well as the regular expenses of pharmaceutical. Our goal is to focus on a particular time frame T in order to accommodate a limited treatment strategy. The following is the definition of the control challenges:$(u_1(t),\ u_2(t),\ u_3(t))$, which fulfill

$$J(u_1^*(t),\ u_2^*(t),\ u_3^*(t)) = min(J(u_1(t),\ u_2(t),\ u_3(t)) : u_1,\ u_2,\ u_3 \in \mathbb{F}),$$

in which
$\mathbb{F} = ((u_1,\ u_2,\ u_3)$ are lebesgue measurable with, $0 \le u_1(t) \le 1,\ 0 \le u_2(t) \le 1,$
$0 \le u_3(t) \le 1,\ t \in [0,\ T])$.

The Evaluation of Existence and Boundedness for Optimum Control

Applying the findings from [36] and [37], I firstly establish that solutions for the control model (9) have boundaries for a finite span of duration. In this regard, I investigate the solutions for its entirety within the current state equations.

Theorem 3. *Assume that* $Y^* = [T^*,\ I^*,\ M^*,\ U^*,\ P^*]^T$ *using initial condition of model (1) and* $\mathbb{F}$ *stands for the controlling set formed over* $[0,\ T]$*.Otherwise put,* $\mathbb{F} = \{(u_1,\ u_2,\ u_3)$ *are measured,*
$0 \le u_1(t) \le 1,\ 0 \le u_2(t) \le 1,\ 0 \le u_3(t) \le 1\}$. *These presumptions are made:*

(i) The associated variables, their starting conditions, including the acceptable controlling set $\mathbb{F}$ *are not empty.*

(ii) The controlling set $\mathbb{F}$ *satisfies the characteristics to be convex and closed.*

(iii) The R.H.S of the mathematical state equations is constrained by the linear combination of conditions and state parameters.

(iv) The integrand of the cost operational in equation (6) has become convex and bounded below.

(v) Since the cost function in equation (10) is satisfied by the positive factors $n_1,\ n_2,$ *and* $\varsigma > 1$*, then* $J = (u_1,\ u_2,\ u_3) \ge n_1 + n_2\left(|u_1|^2 + |u_2|^2 + |u_3|^2\right)^{\frac{\varsigma}{2}}$.
After that, the optimum solution is $(Y^*,\ u_1^*,\ u_2^*,\ u_3^*) \in \mathbb{F}^{1,\infty}\left([0,T],\mathbb{R}_+^5\right) \times L^{\infty}\left([0,T],\mathbb{R}_+^3\right)$ *with the most most optimal result (9) and (10). The equation* $J(u_1^*,\ u_2^*,\ u_3^*) = min\left\{J(u_1,\ u_2,\ u_3) :\ \ u_1, u_2, u_3 \in \mathbb{F}\right\}$ *is satisfied by this solution.*

Proof: It is essential to prove the existence of solutions to the system (9) to meet the given conditions. Since every boundary are satisfied by the controls $(0,\ 0,\ 0)$, control set $\mathbb{F}$ remains non empty. Additionally, set $\mathbb{F}$ serves as a convex, along with a closed subset of L^{∞}. For every equation, I set bounds:

$$\frac{dT}{dt} \leq rT, \quad \frac{dI}{dt} \leq \alpha I, \quad \frac{dM}{dt} \leq \delta + \theta I, \quad \frac{dU}{dt} \leq u_2 \leq 1, \quad \frac{dP}{dt} \leq u_3 \leq 1.$$

The matrix representation of structure (6) is provided by this expression:

$$\begin{pmatrix} \dot{T} \\ \dot{I} \\ \dot{M} \\ \dot{U} \\ \dot{P} \end{pmatrix} \leq \begin{pmatrix} T & 0 & 0 & 0 & 0 \\ 0 & \alpha & 0 & 0 & 0 \\ 0 & \theta & 0 & 0 & 0 \\ 0 & 0 & 0 & 0 & 0 \\ 0 & 0 & 0 & 0 & 0 \end{pmatrix} \begin{pmatrix} T \\ I \\ M \\ U \\ P \end{pmatrix} + \begin{pmatrix} 0 \\ 0 \\ \delta \\ u_2 \\ u_3 \end{pmatrix} = Z_1 Y + Z_2,$$

where

$$Z_1 = \begin{pmatrix} T & 0 & 0 & 0 & 0 \\ 0 & \alpha & 0 & 0 & 0 \\ 0 & \theta & 0 & 0 & 0 \\ 0 & 0 & 0 & 0 & 0 \\ 0 & 0 & 0 & 0 & 0 \end{pmatrix}, \quad Z_2 = \begin{pmatrix} 0 \\ 0 \\ \delta \\ u_2 \\ u_3 \end{pmatrix}.$$

Model (9) has uniformly bounded parameters over a limited period, implying that its solution has also uniform bounds. Additionally, using the bilinear format, the model (9) can be expressed as follows.

$$f(t,\ Y(t), u_1,\ u_2,\ u_3) = \eta(t,\ Y) + u_1 + u_2 + u_3 + \delta,$$

in which η represents an array valued function of $Y(t)$ while $Y(t) = [T,\ I,\ M,\ U,\ P]^T$ be the column vector. I arrive at the following conclusion by taking the fact that a solution for model (9) is bounded.

$$\begin{aligned} |f(t,\ Y(t), u_1,\ u_2,\ u_3)| &\leq |Z_1 Y(t) + |N_2| + |u_1| \\ &\leq k_1 |Y| + |\delta| + |u_2| + |u_3| + |u_1|. \end{aligned}$$

At this instance, the structure's (9) coefficients determine a value for k_1. To determine the integrand's convexity for its cost functional $J(t, Y, \mathbf{u})$, it must be shown $(1-l)J(t, Y, \mathbf{u}) + lJ(t, Y, \boldsymbol{\nu}) \geq J(t, Y, (1-l)\mathbf{u} + l\boldsymbol{\nu})$, where $J(t, Y, \mathbf{u}) = T - M + \frac{1}{2}\sum_{i=1}^{3} \varrho_i k_i^2; \varrho_1 k_1^2 = w_1 u_1^2, \varrho_2 k_2^2 = w_2 u_2^2, \varrho_3 k_3^2 = w_3 u_3^2$, in which $\mathbf{u} = (u_1,\ u_2,\ u_3)$, $\boldsymbol{\nu} = (\nu_1,\ \nu_2,\ \nu_3)$ represents two control vectors and $l = (0,\ 1)$.
Then, $(1-l)J(t, Y, \mathbf{u}) + lJ(t, Y, \boldsymbol{\nu}) = T - M + \frac{1}{2}(1-l)\sum_{i=1}^{3} \varrho_i k_i^2 + \frac{1}{2} l \sum_{i=1}^{3} \varrho_i h_i^2$,
Also $J(t, Y, (1-l)\mathbf{u} + l\boldsymbol{\nu}) = T - M + \frac{1}{2}(1-l)^2 \sum_{i=1}^{3} \varrho_i k_i^2 + \frac{1}{2} l^2 \sum_{i=1}^{3} \varrho_i h_i^2 + (1-l) l \sum_{i=1}^{3} \varrho_i h_i k_i$,

So that, $(1-l)J(t,Y,\mathbf{u}) + lJ(t,Y,\boldsymbol{\nu}) - J(t,Y,(1-l)\mathbf{u}+l\boldsymbol{\nu})$

$$= \frac{1}{2}\sum_{i=1}^{3} \varrho_{i=1}\left\{(l-l^2)k_i^2 + (l-l^2)h_i^2 - 2(1-l)l\sum_{i=1}^{3} h_i k_i\right\}$$
$$= \frac{1}{2}\sum_{i=1}^{3} \varrho_{i=1}\left\{\sqrt{l(l-l)k_i} - \sqrt{l(l-l)h_i}\right\} > 0.$$

Thus, the cost function has become convex. Moreover, $J(u_1,u_2,u_3) \geq T + \frac{1}{2}(w_1u_1^2 + w_2u_2^2 + w_3u_3^2) \geq n_1 + n_2\left(|u_1|^2 + |u_2|^2 + |u_3|^2\right)^{\frac{\varsigma}{2}}$, wherein $\varsigma > 1,\ n_1 > 0$ according to the lower limit of T and $n_2 = \min\{w_1,\ w_2,\ w_3\}$.

6.1. The Hamiltonian

It is shown by (10) that there is an optimum control issue for cost minimization. Our next step is to create a differential formulation of the adjoint variables by using Pontryagin's principle [38]. It is accomplished by developing an enhanced Hamiltonian functional that correlates with the state limitation to determine the optimality of the entire system, as described here:

$$\mathbb{H} = T - M + \frac{1}{2}\left(w_1u_1^2 + w_2u_2^2 + w_3u_3^2\right) + \lambda_1\frac{dT}{dt} + \lambda_2\frac{dI}{dt} + \lambda_3\frac{dM}{dt} + \lambda_4\frac{dU}{dt} + \lambda_5\frac{dP}{dt},$$

Where $\lambda' s$ are the variables that collaborate with the system's state factors.

$$\mathbb{H} = T - M + \frac{1}{2}\left(w_1u_1^2 + w_2u_2^2 + w_3u_3^2\right) + \lambda_1\left(rT\left(1-\frac{T}{K_T}\right) - \beta TI - N_T(1-e^{-P})T - \gamma TM - UT\right)$$
$$+ \lambda_2\left(\frac{\alpha IT}{T+K_I} - \phi IT - \mu I - N_I\left(1-e^{-P}\right)I\right) + \lambda_3\left(\delta - \eta M + \theta I - u_1(t)M\right) + \lambda_4\left(-\chi U + u_2(t)\right)$$
$$+ \lambda_5\left(-\sigma P + u_3(t)\right).$$

I obtain the adjoint solution along with the transversality conditions by applying Pontryagain's principle [38], which lead to

$$\frac{d\lambda_1}{dt} = -\left[1 + \lambda_1\left(r\left(1-\frac{2T}{K_T}\right) - \beta I - N_I\left(1-e^{-P}\right) - \gamma M - U\right) + \lambda_2\left(\frac{K_I\alpha I}{(T+K_I)^2} - \phi I\right)\right],$$
$$\frac{d\lambda_2}{dt} = \lambda_1\beta T - \lambda_2\left(\frac{\alpha T}{T+K_I} - \phi T - \mu - N_I(1-e^{-P})\right) - \lambda_3\theta,$$
$$\frac{d\lambda_3}{dt} = 1 + \lambda_1\gamma T + \lambda_3(\eta + u_1(t)),$$
$$\frac{d\lambda_4}{dt} = \lambda_1 T + \lambda_4\chi,$$
$$\frac{d\lambda_5}{dt} = \lambda_1 T N_T e^{-P} + \lambda_2 I N_I e^{-P} + \lambda_5\sigma.$$

Theorem 4. *When optimal model (9) is applied to a control set* $\mathbb{F}$*, the control set* $(u_1^*,\ u_2^*,\ u_3^*)$*. which minimizes the cost function* J*, is provided as follows:*

$$u_1^*(t) = \min\left(1,\ max\left(0,\ \frac{\lambda_3 M}{w_1}\right)\right),$$
$$u_2^*(t) = \min\left(1,\ max\left(0,\ \frac{-\lambda_4}{w_2}\right)\right),$$
$$u_3^*(t) = \min\left(1,\ max\left(0,\ \frac{-\lambda_5}{w_3}\right)\right).$$

Proof: The optimum states having controlling state equations, represented by the symbols $(Y^*,\ u_1^*,\ u_2^*,\ u_3^*)$, are provided in (9). The description of the starting values with $Y = [T,\ I,\ M,\ U,\ P]$ is as follows: $Y^*(t) = Y_0(t)$ for all $t \in [0, T]$ along with $\lambda_1(T) = \lambda_2(T) = \lambda_3(T) = \lambda_4(T) = \lambda_5(T) = 0$. In relation to a control combination $(u_1^*,\ u_2^*,\ u_3^*)$, its Hamiltonian is optimized by using transversality requirements.

$$\frac{\partial \mathbb{H}}{\partial u_1} = w_1 u_1 - \lambda_3 M = 0 \Longrightarrow \frac{\lambda_3 M}{w_1} = \tilde{u}_1,$$
$$\frac{\partial \mathbb{H}}{\partial u_2} = w_2 u_2 + \lambda_4 = 0 \Longrightarrow \frac{-\lambda_4}{w_2} = \tilde{u}_2,$$
$$\frac{\partial \mathbb{H}}{\partial u_3} = w_3 u_3 + \lambda_5 = 0 \Longrightarrow \frac{-\lambda_5}{w_3} = \tilde{u}_3.$$

Here is how I clarify these controls:

$$u_1^* = \begin{cases} 0 \ \text{ if } \tilde{u}_1 \leq 0, \\ \tilde{u}_1 \ \text{ if } \tilde{u}_1 < 0 < 1, \\ \tilde{u}_1 \ \text{ if } \tilde{u}_1 \geq 1. \end{cases}$$

$$u_2^* = \begin{cases} 0 \ \text{ if } \tilde{u}_2 \leq 0, \\ \tilde{u}_2 \ \text{ if } \tilde{u}_2 < 0 < 1, \\ \tilde{u}_2 \ \text{ if } \tilde{u}_2 \geq 1. \end{cases}$$

Also

$$u_3^* = \begin{cases} 0 \ \text{ if } \tilde{u}_3 \leq 0, \\ \tilde{u}_3 \ \text{ if } \tilde{u}_3 < 0 < 1, \\ \tilde{u}_3 \ \text{ if } \tilde{u}_3 \geq 1. \end{cases}$$

The optimization system incorporated their co-state, also combined state factors, in addition to their original or transversality criteria, by defining the control factors as follows:

$$\begin{aligned}
\frac{dT}{dt} &= rT\left(1-\frac{T}{K_T}\right) - \beta TI - N_T(1-e^{-P})T - \gamma TM - UT,\\
\frac{dI}{dt} &= \frac{\alpha IT}{T+K_I} - \phi IT - \mu I - N_I\left(1-e^{-P}\right)I,\\
\frac{dM}{dt} &= \delta - \eta M + \theta I - \min\left(1,\ max\left(0,\ \frac{\lambda_3 M}{w_1}\right)\right)M,\\
\frac{dU}{dt} &= -\chi U + \min\left(1,\ max\left(0,\ \frac{-\lambda_4}{w_2}\right)\right),\\
\frac{dP}{dt} &= -\sigma P + \min\left(1,\ max\left(0,\ \frac{-\lambda_5}{w_3}\right)\right).
\end{aligned}$$

With $\lambda_1(T) = \lambda_2(T) = \lambda_3(T) = \lambda_4(T) = \lambda_5(T) = 0$ for all $t \in [0,\ T]$, and $T(0) = T_0,\ I(0) = I_0,\ M(0) = M_0,\ U(0) = U_0,\ P(0) = P_0,$, satisfied.

7. Analysis of Cost Effectiveness

This study's cost-effectiveness analysis is carried out using a mathematical modeling approach. The term "cost" refers to a normalized control cost that represents the relative intensity, implementation effort, and potential treatment burden associated with the applied control strategies, such as chemotherapy, radiation therapy, and microbiome regulation, rather than actual financial or clinical expenses. The benefits of health programs or plans are assessed using economic analysis to justify the costs of medical treatments, such as radiation therapy and cancer chemotherapy, as well as antibiotics that kill microorganisms and help eradicate diseases. It is crucial to monitor and manage tumor growth that involves nearby cells. Therefore, it's critical to identify and implement affordable treatment plans to prevent the disease from progressing. A technique for evaluating the advantages and disadvantages of implementing control measures is a cost-effectiveness analysis. I employ these approaches, such as strategy (1), which shows lower intensity of (u_1 lower effort for killing bacteria and u_2 lower dose of radiotherapy). The second strategy is mild intensity of u_1 and u_2. Strategy (3) is an integration of all three controls $u_1,\ u_2$ and u_3 with their higher intensity, and in the last strategy (4), which represents all three controls with maximum effort to control the disease. In this case, I use only these four techniques to analyze cost-effectiveness and disease-prevention robustness. Two cost efficiency ratios are the average **(ACER)** and incremental **(ICER)**. The following is the description of these techniques.

Table 1: Outcomes of the ACER

Strategy	**Normalized Cost** ($)	**Efficiency (%)**	**ACER** ($)
Minimal intensity of (u_1, u_2)	62.14	84.23	0.74
Mildly intense (u_1, u_2)	62.79	89.23	0.70
Extremely intense (u_1, u_2, u_3)	63.24	94.23	0.67
Maximum intensity of (u_1, u_2, u_3)	63.81	99.23	0.64

ACER or Average Cost Efficiency Ratio

It's the proportion of developing cells the method avoids relative to the total cost of the procedures. Thus, the following shows how the (ACER) equation is formatted.

$$\text{ACER} = \frac{\text{Total cost of the strategy j}}{\text{Total tumour cell loss as a result of using strategy j}}.$$

To determine efficiency, I must calculate the total reduction in tumor cells resulting from implementing treatment strategies 1, 2, and 3 throughout the medicinal period T. It can be done by using the formula $F_j = T(0) - T(T)^*$, in which $T(0)$ denotes the quantity of tumour the cells at the beginning of the course of the therapy while $T(T)^*$ denotes the amount of tumour cells after the therapies terms. The entire amount spent during the approach is determined below:

$$\frac{1}{2}\int_0^T (w_1u_1 + w_2u_2 + w_3u_3)dt.$$

The relative burden or intensity of the relevant control measures is represented by the positive weighting factors w_1, w_2, and w_3 in this case; bigger values suggest greater treatment effort or possible side effects.

ICER or Incrementally Cost Efficiency Ratio

If two techniques (i vs. j) are being compared, the ICER measures the greater cost per extra unit. The formula for (ICER) will be:

$$(\text{ICER})_{i,j} = \frac{\text{Cost}_i - \text{Cost}_j}{\text{Effectiveness}_i - \text{Effectiveness}_j}.$$

The findings imply that while moderate-intensity control strategies might offer a good

Table 2: Outcomes of the ICER

Strategy	**Normalized Cost** ($)	**Efficiency (%)**	**ICER** ($)
Minimal intensity of (u_1, u_2)	62.14	84.23	0.74
Mildly intense (u_1, u_2)	62.79	89.23	0.13
Extremely intense (u_1, u_2, u_3)	63.24	94.23	0.09
Maximum intensity of (u_1, u_2, u_3)	63.81	99.23	0.11

compromise between efficacy and control effort, higher-intensity control strategies achieve larger tumor reduction within the modeling framework.

8. Conclusion

A computational model with five compartments that describes the interplay among tumor cells, the immune response, and the microbial population, combined with radiochemotherapy, was described in this paper. The findings show that the microbial bacteria significantly influence the connection between tumor cells and the immune system. By direct contact, they help decrease tumors. For example, they may block or compete with microbes to reduce tumor cell growth. Furthermore, by altering tumor size over time, microorganisms indirectly influence the immune system.

To ensure that the interaction remains biologically relevant, I verified the tumor model's integrity by providing evidence of its existence, positivity, and boundedness. Every therapeutically significant level was identified, including the inner state in which every population remains, a disease-free state, and a state in which only tumor and microbial components remain. I have shown that different constant levels may be obtained under some threshold conditions. It has also been proven that a certain level of chemotherapy can eradicate tumor cells. If this is not possible, tumor growth may be restricted to a certain level, even though radio and chemotherapy damage immune cells due to the microbiome. Metabolites produced by specific gut bacteria improve the body's response to treatments and boost the recovery of immune cells. Hence, despite the immunosuppressive effects of radiochemotherapies, the microbiome enhances immune function and prevents tumor growth. Using a biologically justified, cost-effective approach, an optimal control problem was formulated to minimize toxicity to healthy cells, maintain immunological and microbial populations, and reduce tumor burden at the lowest cost.

The findings highlight the importance of gut microbiota in shaping tumor dynamics and clinical outcomes. According to the study, combining microbial treatments with radiotherapy and chemotherapy may enhance the efficacy of cancer therapies while reducing side effects.

References

[1] P Das, R K Upadhyay, P Das, and D Ghosh. Exploring dynamical complexity in a time-delayed tumor-immune model. *Chaos: An Interdisciplinary Journal of Nonlinear Science*, 30:123118, 2020.

[2] R A Gatenby and P K Maini. Mathematical oncology: Cancer summed up. *Nature*, 421(6921):321–321, 2003.

[3] G P Dunn, A T Bruce, H Ikeda, L J Old, and R D Schreiber. Cancer immunoediting: from immunosurveillance to tumor escape. *Nature Immunology*, 3(11):991–998, 2002.

[4] S I Grivennikov, F R Greten, and M Karin. Immunity, inflammation, and cancer. *Cell*, 140(6):883–890, 2010.

[5] L G de Pillis, W Gu, K R Fister, T A Head, K Maples, A Murugan, and K Yoshida. Chemotherapy for tumors: An analysis of the dynamics and a study of quadratic and linear optimal controls. *Mathematical Biosciences*, 209(1):292–315, 2007.

[6] D Zheng, T Liwinski, and E Elinav. Interaction between microbiota and immunity in health and disease. *Cell Research*, 30(6):492–506, 2020.

[7] A Sivan, L Corrales, N Hubert, J B Williams, K Aquino-Michaels, Z M Earley, and T F Gajewski. Commensal Bifidobacterium promotes antitumor immunity and facilitates anti–PD-L1 efficacy. *Science*, 350(6264):1084–1089, 2015.

[8] M Vétizou, J M Pitt, R Daillère, P Lepage, N Waldschmitt, C Flament, and L Zitvogel. Anticancer immunotherapy by CTLA-4 blockade relies on the gut microbiota. *Science*, 350(6264):1079–1084, 2015.

[9] P P Escriva, C C T Bernardino, and E Letellier. De-coding the complex role of microbial metabolites in cancer. *Cell Reports*, 44(3):115358, 2025.

[10] Kamel Guedri, Yasir Ramzan, Amna Riaz, Hatoon Abdullah Niyazi, Basim M Makhdoum, and Aziz Ullah Awan. A mathematical framework for integrating epidemic dynamics and intervention strategies to mitigate hearing loss from lassa virus. *International Journal of Biomathematics*, 2025.

[11] Yasir Ramzan, Kamel Guedri, Aziz Ullah Awan, Jeevan Kafle, Hatoon A Niyazi, and Basim M. Makhdoum. Modeling gonorrhea and hiv coinfection with predictive analytics for disability and mortality risks. *Scientific Reports*, 15(1):32983, 2025.

[12] Kamel Guedri, Yasir Ramzan, Muhammad Mudassar Bilal, Hatoon Abdullah Niyazi, Aziz Ullah Awan, and Basim M Makhdoum. Gender-specific modeling for lassa virus transmission with hearing loss disability risk and control strategies. *European Journal of Pure and Applied Mathematics*, 18(2):6104–6104, 2025.

[13] Yasir Ramzan, Amna Riaz, Kamel Guedri, Aziz Ullah Awan, Hatoon A Niyazi, Hanadi Alzubadi, and Basim M Makhdoum. A nonlinear optimization framework for a lassa fever model capturing zoogenic transmission and disability risks. *The European Physical Journal Plus*, 140(10):975, 2025.

[14] Kamel Guedri, Yasir Ramzan, Aziz Ullah Awan, Bandar M Fadhl, and Mowffaq Oreijah. Modeling transmission patterns and optimal control through nanotechnology: A case study of malaria causing brain disabilities. *Journal of Disability Research*, 3(1):20230061, 2024.

[15] Yasir Ramzan, Bandar M Fadhl, Shafiullah Niazai, Aziz Ullah Awan, and Kamel Guedri. Decoding the transmission and subsequent disability risks of rabineurodeficiency syndrome without recuperation. *Scientific Reports*, 15(1):17322, 2025.

[16] A U Awan, T Hussain, K O Okosun, and M Ozair. Qualitative analysis and sensitivity based optimal control of pine wilt disease. *Advances in Difference Equations*, 2018(1):27, 2018.

[17] M Ozair, T Hussain, X Shi, F Tasneem, and J F Gómez-Aguilar. Dynamical features of pine wilt disease model with asymptotic carrier. *The European Physical Journal Plus*, 135(4):366, 2020.

[18] T Hussain, A U Awan, K A Abro, M Ozair, and M Manzoor. A mathematical and parametric study of epidemiological smoking model: a deterministic stability and optimality for solutions. *The European Physical Journal Plus*, 136(1):11, 2021.

[19] A Szabó and R M Merks. Cellular potts modeling of tumor growth, tumor invasion, and tumor evolution. *Frontiers in Oncology*, 3:87, 2013.

[20] S Zuppone, C Assalini, C Minici, O A Botrugno, F Curnis, M Degano, and R Vago. A novel rgd-4c-saporin conjugate inhibits tumor growth in mouse models of bladder cancer. *Frontiers in Oncology*, 12:846958, 2022.

[21] A Radunskaya, R Kim, and T Woods II. Mathematical modeling of tumor immune interactions: A closer look at the role of a pd-l1 inhibitor in cancer immunotherapy. *Spora: A Journal of Biomathematics*, 4(1):25–41, 2018.

[22] P Unni and P Seshaiyer. Mathematical modeling, analysis, and simulation of tumor dynamics with drug interventions. *Computational and Mathematical Methods in Medicine*, 2019(1):4079298, 2019.

[23] G Song, T Tian, and X Zhang. A mathematical model of cell-mediated immune response to tumor. *Mathematical Biosciences and Engineering*, 18(1):373–385, 2021.

[24] P Das, S Das, P Das, F A Rihan, M Uzuntarla, and D Ghosh. Optimal control strategy for cancer remission using combinatorial therapy: a mathematical model-based approach. *Chaos, Solitons & Fractals*, 145:110789, 2021.

[25] B Dhar, P K Gupta, and A Yildirim. Dynamical behaviour of a tumour-immune model focusing on the dosage of targeted chemotherapeutic drug. *International Journal of Computer Mathematics*, 99(12):2568–2582, 2022.

[26] M Sardar, S Khajanchi, and B Ahmad. A tumor–immune interaction model with the effect of impulse therapy. *Communications in Nonlinear Science and Numerical Simulation*, 126:107430, 2023.

[27] A Kumar, U S Dubey, and B Dubey. The impact of radio-chemotherapy on tumour cells interaction with optimal control and sensitivity analysis. *Mathematical Biosciences*, 369:109146, 2024.

[28] W Qin, Y Zhao, and J Yang. Modeling the effects of obesity on a tumor-immune model with combined therapy. *Mathematics and Computers in Simulation*, 233:276–295, 2025.

[29] S Kumar, R P Chauhan, A H Abdel-Aty, and S F Abdelwahab. A study on fractional tumour–immune–vitamins model for intervention of vitamins. *Results in Physics*, 33:104963, 2022.

[30] S Kumar, R P Chauhan, A A Aly, S Momani, and S Hadid. A study on fractional hbv model through singular and non-singular derivatives. *The European Physical Journal Special topics*, 231(10):1885–1904, 2022.

[31] M Naim, A Zeb, A A Mohsen, Y Sabbar, and M Yıldız. Local and global stability of a fractional viral infection model with two routes of propagation, cure rate and non-lytic humoral immunity. *Mathematical Modelling and Numerical Simulation with Applications*, 4(5-Special Issue: ICAME'24):94–115, 2024.

[32] S K Shafeeq, M M Abdulkadhim, A A Mohsen, H F Al-Husseiny, and A Zeb. Bifurcation analysis of a vaccination mathematical model with application to covid-19 pandemic. *Communications in Mathematical Biology and Neuroscience*, 2022:86, 2022.

[33] R M Yaseen, N F Ali, A A Mohsen, A Khan, and T Abdeljawad. The modeling and mathematical analysis of the fractional-order of cholera disease: Dynamical and simulation. *Partial Differential Equations in Applied Mathematics*, 12:100978, 2024.

[34] L G De Pillis and A Radunskaya. A mathematical tumor model with immune resistance and drug therapy: An optimal control approach. *Computational and Mathematical Methods in Medicine*, 3(2):79–100, 2001.

[35] S N Gardner. A mechanistic, predictive model of dose-response curves for cell cycle phase-specific and-nonspecific drugs. *Cancer Research*, 60(5):1417–1425, 2000.

[36] W H Fleming and R W Rishel. *Deterministic and stochastic optimal control.* Springer-Verlag, New York, Heidelberg, Berlin, 2012.

[37] D L Lukes. *Differential equations: Classical to controlled.* Academic Press Inc., New York, London, 1982.

[38] L S Pontryagin. *Mathematical theory of optimal processes.* Gordon and Breach Science Publishers, New York, London, Paris, Montreux, Tokyo, 2018.